J Mol Med (2015) 93:187–198
DOI 10.1007/s00109-014-1213-7

JMolMed

ORIGINAL ARTICLE

# The anti-angiogenic role of discoidin domain receptor 2 (DDR2) in laser-induced choroidal neovascularization

**Tong Zhu · Jie Zhu · Xin Bu · Hu Zhao · Shuya Zhang · Yuan Chang · Rong Li · Libo Yao · Yusheng Wang · Jin Su**

Received: 6 February 2014 / Revised: 17 August 2014 / Accepted: 21 August 2014 / Published online: 30 October 2014


**Abstract**
Choroidal neovascularization (CNV), an aberrant growth of blood vessels in the choroid layer of the eye, is a major cause of vision loss. In view of our recent finding that discoidin domain receptor 2 (DDR2), a collagen-binding receptor tyrosine kinase, is involved in control of vascular endothelial activity and tumor angiogenesis, the present study aims to investigate whether and how DDR2 affects the pathogenesis of CNV. We initially found that a spontaneous DDR2 mutant mouse colony (*slie*) exhibited enhanced amplitude of laser-induced CNV. The inhibitory role of DDR2 in CNV development was further confirmed by experiments through intravitreous injection of DDR2 small interference RNA (siRNA) or DDR2-expressing adenovirus. Quantitative real-time polymerase chain reaction (qPCR) and immunoblot analysis showed that DDR2 regulates the expression of several major pro-angiogenic factors in the laser-injured choroid as well as in retinal pigment epithelium (RPE) cells. In addition, it was demonstrated that the CNV-induced increases in the phosphorylation levels of Akt and mTOR were affected by the upregulation or downregulation of DDR2. Thus, the data from this study for the first time revealed that DDR2 negatively regulates the development of experimental CNV in vivo, which may provide a novel target for preventing human pathological ocular neovascularization.

**Key messages**
- DDR2 does not affect retinal development.
- DDR2 inhibits laser-induced CNV.
- DDR2 regulates angiogenic factor expression in CNV lesion as well as in RPE cells.
- DDR2 is involved in modulation of CNV-induced activation of PI3K pathway.

**Keywords** DDR2 · Choroidal neovascularization · Collagen receptor · Extracellular matrix

Tong Zhu and Jie Zhu and Xin Bu equally contribute to this paper.

**Electronic supplementary material** The online version of this article (doi:10.1007/s00109-014-1213-7) contains supplementary material, which is available to authorized users.

T. Zhu · J. Zhu · Y. Chang · R. Li · Y. Wang (✉)
Department of Ophthalmology, Xijing Hospital, The Fourth Military Medical University, 169 Changle Western Road, Xi'an 710032, China
e-mail: wangys003@126.com

X. Bu · H. Zhao · L. Yao · J. Su (✉)
State Key Laboratory of Cancer Biology, Department of Biochemistry and Molecular Biology, The Fourth Military Medical University, 169 Changle Western Road, Xi'an 710032, China
e-mail: sujin923@fmmu.edu.cn

S. Zhang
Key Laboratory of Fertility Preservation and Maintenance of Ministry of Education, Department of Biochemistry and Molecular Biology, Ningxia Medical University, Yinchuan, China

R. Li
Affiliated hospital of Xi'an Medical University, Xi'an 710077, China

## Introduction

Choroidal neovascularization (CNV), a process involving the growth of new blood vessels from the choriocapillaris across the retinal pigment epithelium (RPE) layer and Bruch's membrane and their extension into the subretinal space, is a major feature of several ocular diseases that cause vision loss, such as wet age-related macular degeneration (AMD), ocular histoplasmosis syndrome, and pathological myopia [1, 2]. The etiology of CNV is multifactorial and complicated, and a number of genetic and environmental factors have been cited as possible risk factors for its formation [3].

Increasing amounts of evidences indicate that inflammatory and angiogenic events coordinately determine the development of CNV via upregulation of a variety of diffusible cytokines, such as vascular endothelial growth factor (VEGF) and tumor necrosis factor (TNF)-α [4, 5]. The identification of the predominant role of VEGF in promoting CNV formation has led to the application of anti-VEGF therapy as a useful treatment option for intraocular neovascular disorders [6, 7]. Stimulators other than the soluble factors, the insoluble extracellular matrix (ECM) also plays crucial roles in controlling angiogenesis. Integrins represent a class of cell surface receptors that can mediate the signaling from ECM to the cell interior. It has been reported that the blockade of several subtypes of integrins is effective in inhibiting experimental CNV [8–10].

In contrast to integrins that lack enzymatic activities, discoidin domain receptors (DDRs), consisting of DDR1 and discoidin domain receptor 2 (DDR2), use collagens as their cognate ligands and are tyrosine phosphorylated upon activation [11]. DDR2 can regulate cell proliferation, differentiation, invasion, and migration [12]. By use of genetic mouse models, DDR2 was demonstrated to be associated with several human pathological processes including osteoarthritis, wound healing, hepatic fibrosis, as well as tumor metastasis [13–16]. Recently, the data from our lab showed that DDR2 is a critical regulator of endothelial activity as well as tumor angiogenesis [17]. These findings stimulated our interest to investigate whether DDR2 similarly plays a role in the pathogenesis of CNV.

In this work, we initially found that DDR2 mutant mice were more prone to induction of laser-induced CNV than wild-type animals. This result was further supported by the intravitreal application of DDR2 small interference RNA (siRNA) and DDR2-expressing adenovirus. It was also shown that the expression levels of major pro-angiogenic factors and the activation status of PI3K/Akt/mTOR pathway in the injured choroidal tissues were consistent with the severity of CNV. Therefore, our current study suggests that enhanced expression of DDR2 might be used as a potential strategy to treat CNV.

## Materials and methods

### Animals and cell line

The heterozygous *slie* mouse colony with deletion mutation of *Ddr2* gene was purchased from Jackson Laboratory (Bar Harbor, ME, USA) and used to generate homozygotes [18]. The genotyping of all mice was performed by quantitative real-time polymerase chain reaction (qPCR) with TaqMan probes on ABI 7500 (Applied Biosystems, Foster City, CA, USA) according to the providers' instructions. Animals were housed under pathogen-free conditions, and all animal experiments were performed in strict adherence to the ARVO Statement for the Use of Animals in Ophthalmic and Vision Research. Human RPE cell line ARPE19 (ATCC, Manassas, VA, USA) was maintained in 1640 medium (Invitrogen, Carlsbad, CA, USA) supplemented with 15 % fetal bovine serum (FBS).

### Mouse model of CNV

CNV was generated by laser photocoagulation-induced rupture of Bruch's membrane as described previously [19]. Briefly, 6 to 8-week wild-type or homozygous slie mutant mice were anesthetized through intraperitoneal injection of 0.5 % sodium pentobarbital (45 mg/kg BW), and the pupils were then dilated with 1 % tropicamide. The 532 nm laser irradiation was applied on one randomly selected eye of each animal with a duration of 0.1 s and an intensity of 90 mW so as to produce a spot size of 75 μm. In each eye, six focal laser photocoagulation lesions were placed at positions that were 1.5–2 disc diameters away from the optic nerve. The production of a bubble at the time of laser insult was considered to indicate the rupture of Bruch's membrane.

### Intravitreal treatment with siRNA, adenovirus, or PI3K inhibitor

Intravitreal injection of siRNA, adenovirus, and PI3K inhibitor LY294002 (Cell signaling) was performed under an operating microscope. Recombinant adenovirus expressing enhanced green fluorescent protein (EGFP) or full-length DDR2 was packaged and purified by Vector Gene Technology Company (Beijing, China) and administered to the mice at $1\times10^9$ *pfu* per mouse. The expression of Ad-DDR2 has been confirmed by our lab previously [17]. For in vivo silencing of DDR2 in the mouse eye, a nonspecific control siRNA or DDR2-specific siRNA was modified with 2′-methoxy (2′-OMe) by GenePharma Company (Shanghai, China) to improve stability. The sense sequences of siRNAs are as follows: DDR2, 5′-TTGA GATGAATACTAGCTTAG-3′and control, 5′-TTCTCCGA ACGTGTCACGTT-3′. The silencing effect of DDR2 siRNA has been validated by our previous in vitro study [20]. Two microliters of siRNA duplex (100 μg/ml) was used to treat a mouse. For treatment with PI3K inhibitor, each mouse received 2 μL of a stock solution of LY294002 (3 mM) or dimethyl sulfoxide (DMSO).

### Transmission electron microscopy (TEM)

The mouse eyes were enucleated and fixed in 2.5 % glutaraldehyde in cacodylate buffer at room temperature for 12 h, followed by post-fixation, dehydration, and embedding in

Epon-araldite. Semi-thin section (1 μm) through the optic nerve was prepared, stained with toluidine blue, and examined by light microscopy. Ultrathin section (0.5 μm) of selected areas was then prepared and double-stained with uranyl acetate and lead citrate for electron microscopy (CM-12 TEM; Philips). We used at least ten digital images for each sample to measure the thickness of Bruch's membrane at a magnification of ×20,000. A transparent grid was superimposed onto the micrograph, with RPE basement membrane aligned with the horizontal line. Five random measurements were made on each digital image using Image J software.

### Fluorescein dextran perfusion of the retinal blood vessels

Anesthetized mice were perfused with 1 ml of fluorescein-conjugated dextran (molecular weight 2,000,000; 50 mg/ml; Sigma) in 4 % phosphate-buffered saline through the left ventricle of the heart. The eyes were then enucleated and fixed in 4 % paraformaldehyde for 3 h. Under a dissecting microscope, the retina was removed and flat mounted on a glass slide covered with a coverslip after a few drops of glycerinum were placed on the slide. The retinas were photographed under a fluorescence microscope. Vessel density was measured by counting branchpoint number in randomly selected fields (1200 μm×1200 μm, five fields per retina).

### Evaluation of CNV severity

The size of CNV was evaluated 14 days after laser photocoagulation by fundus fluorescence angiography (FFA), choroidal flat-mount, and histopathological examination. For FFA assay, the mice received intraperitoneal injections of 0.1 ml 2.5 % sodium fluorescein (Wuzhou Pharmaceutical, Guangxi, China) after anesthetization and 2 min after the injection, the fluorescent signal was recorded with a digital imaging system (Heidelberg Engineering, Heidelberg, Germany). The leakage of CNV was graded by two examiners independently using reference angiograms as follows: 0: no leakage; 1: slight leakage (minimum leakage or a staining of tissue with no leakage); 2: moderate leakage (small but evident leakage of less than one-quarter disc area); and 3: prominent leakage (large evident leakage with hyperfluorescence increasing in intensity and in size).

Choroidal flat-mount analysis was used to determine the area and volume of CNV in accordance with our previously described protocol [21]. Briefly, the anesthetized mice were transcardially perfused with a 0.9 % saline solution followed by a 4 % paraformaldehyde solution. The entire ocular globes were enucleated, and the anterior segment and the neural retina were carefully removed. The remaining RPE-choroid-sclera complex was flat mounted by five radial cuts and then permeabilized in 0.2 % Triton X-100 solution for 24 h. Choroidal preparations were incubated with a 1:1000 solution of rhodamine-conjugated agglutinin (Vector Laboratories, Burlingame, CA, USA) for another 24 h followed by wash in 0.01 M Tris-Buffered Saline Tween-20 (TBST) solution. The fluorescence signal of rhodamin was taken by a confocal laser-scanning microscope (FluoView FV-1000; Olympus). The area of CNV was measured by Image-Pro Plus (Media Cybernetics, Carlsbad, CA, USA). The volume of CNV was evaluated through three-dimensional reconstruction of the images by Imaris software.

For histopathological examination, the mouse eyes were fixed in Bouin's solution after enucleation. The eyecups were then generated as previously described [22]. After paraffin embedding, 4-μm serial sections were prepared for hematoxylin-eosin (HE) staining. The length and thickness of each CNV were calculated by Image-Pro Plus 6.0. Ten lesions of each group were selected for a statistical analysis.

### Quantitative real-time PCR (qPCR)

For each group, three eyecups were pooled together to isolate RNA using Trizol (Takara, Kyoto, Japan). Complementary DNA (cDNA) was synthesized with a commercial kit (TaKaRa). qPCR was conducted on ABI 7500 using the SYBR Green (TaKaRa). The primer sequences for mouse genes were as follows: *Gapdh* (forward: TGACCACAGTCCATGCCATA ; reverse: GACGGACACATTGGGGGTAG); *Vegfa* (forward: ACTGGACCCTGGCTTTACTG; reverse: CACAGGACGG CTTGAAGAT); *Ang-2* (forward: CACAGCGAGCAGCTAC AGTC; reverse: ATAGCAACCGAGCTCTTGGA); and *Fgf2* (forward: CGTCAAACTACAACTCAAGCA; reverse: CGTC CATCTTCCTTCATAGCA). Data analysis was completed by ABI Prism 7500 SDS software package.

### Immunoblot

For each group, three homogenized eyecups were lyzed in RIPA buffer (0.05 M Tris-HCl pH 7.4, 0.15 M NaCl, 0.25 % deoxycholic acid, 1 % NP-40, 1 mM EDTA, 1 mM phenylmethylsulfonyl fluoride, 1 μg/ml aprotinin, 1 μg/ml leupeptin, and PhosSTOP) to obtain the protein extracts. Fifty micrograms of total proteins were resolved by 10 % SDS polyacrylamide gel electrophoresis (SDS-PAGE) and transferred to Hybond-ECL nitrocellulose membranes (Amersham Biosciences). After blocking in Tris-buffered saline containing 5 % skim milk and 0.1 % Tween-20, the membranes were incubated with primary antibodies, followed by incubation with horseradish peroxidase (HRP)-conjugated secondary antibodies. The addition of chemi-luminescent HRP substrate solution (Millipore, USA) was used to develop the images. The following primary antibodies were used: mouse anti-DDR2 (R&D systems, USA), rabbit polyclonal anti-VEGF (Abcam, USA) and anti-Ang-2 (Cell Signaling Technology), mouse anti-Akt/pAkt (Cell Signaling Technology), anti-mTOR/pmTOR (Ser2448) (Cell Signaling Technology), and

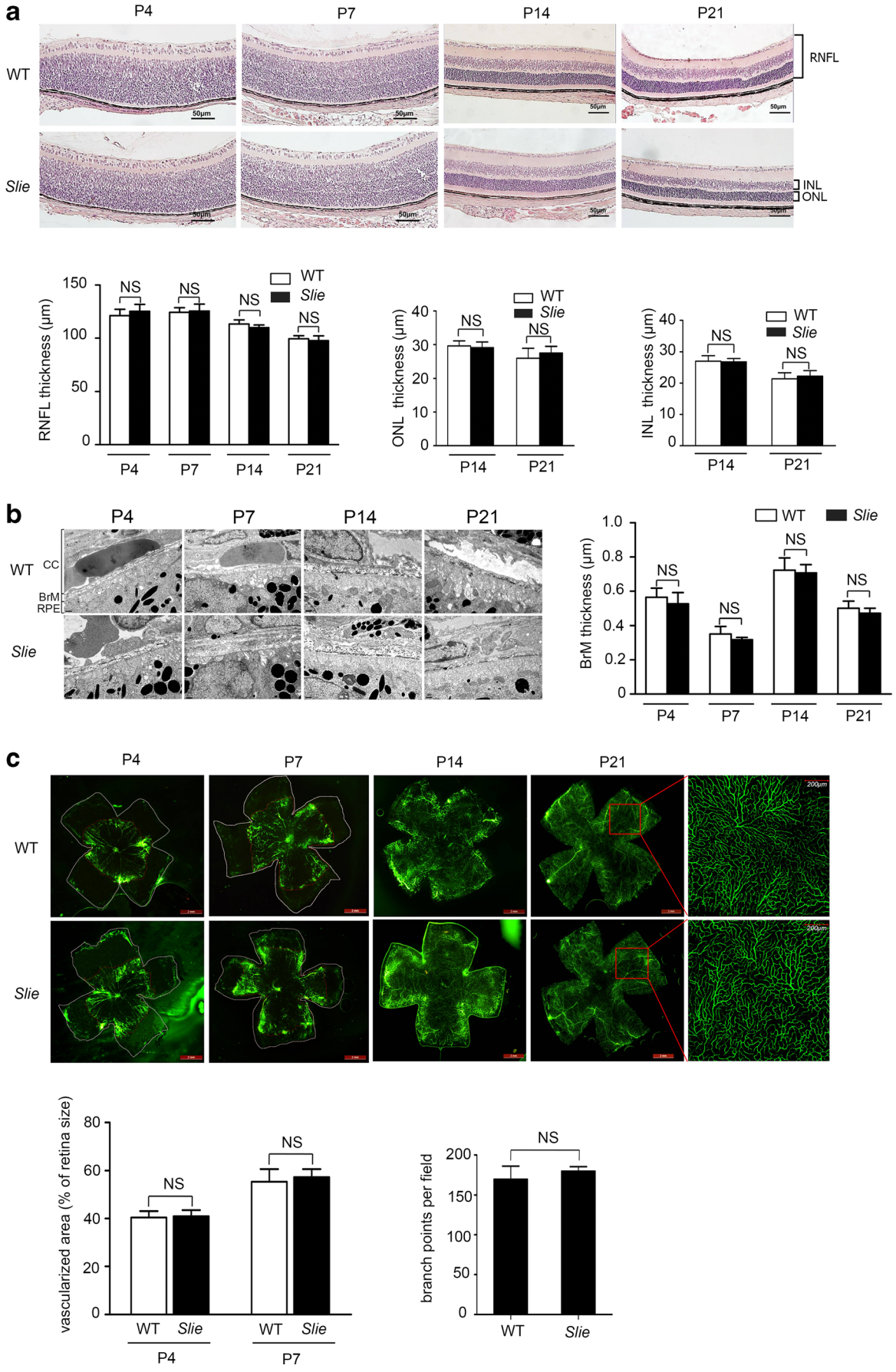
a
P4
P7
P14
P21
WT
Slie
RNFL
INL
ONL
50μm
RNFL thickness (μm)
150
100
50
0
NS
WT
Slie
ONL thickness (μm)
40
30
20
10
INL thickness (μm)
b
CC
BrM
RPE
BrM thickness (μm)
1.0
0.8
0.6
0.4
0.2
c
200μm
vascularized area (% of retina size)
80
60
40
20
branch points per field
200
150
100

◀ **Fig. 1** DDR2 deficient mice are normal in subretinal morphology. H&E staining (**a**) of the eyes from wild-type or slie mutant mice at the indicated postnatal days. *Scale bar*, 50 μm. Histograms show the thickness of retinal nerve fibre layer (RNFL), inner nuclear layer (INL), and outer nuclear layer (ONL), respectively. Representative transmission electron micrograph of the subretinal region of wild-type or slie mice (**b**). *Scale bar* = 0.5 μm. Histogram indicates the average thickness of the Bruch's membrane in three mice. The retinal blood vessels visualized by fluorescein-conjugated dextran (**c**). *Left* histogram represents quantification of the retinal vascularized area at postnatal days 4 and 7. *Right* histogram shows quantification of the branch points per field at postnatal day 21. NS=no significance

anti-β-actin (1:1000). All experiments were repeated at least three times.

### Statistical analysis

Statistical analyses were performed using SPSS software program. Data from several experiments were pooled and subsequently presented as the means and standard deviations. One-way analyses of variance (ANOVAs) followed by LSD-*t* tests were used to make comparisons between pairs of groups. Student's *t* test was used to examine the differences between the two groups of data. All of the experimental datasets were scrutinized to ensure that the sample variance was normally distributed, and appropriate nonparametric tests were applied when necessary. A two-tailed $p$ value of $<0.05$ was considered significant.

## Results

### DDR2 deficient mice appear normal in the structure of subretinal region and in the retinal vascular development

It is necessary to examine whether DDR2 affects the structure of the posterior segment of the eye before investigating its role in the pathological conditions. To this end, we performed H&E and ultrastructural analysis of the eye from control and DDR2 mutant mice (*slie*) at different time points after birth. The results showed that the animals between the two groups did not differ in the thickness of either each retinal layer or Bruch's membrane (Fig. 1a, b). In addition, the development of retinal vasculature was also not influenced by a host deficiency of DDR2 (Fig. 1c).

### The expression profile of DDR2 in the choroidal tissues of mice in response to laser photocoagulation

To investigate the involvement of DDR2 in CNV, we examined its expression profile during the phase of laser-injured CNV. At the indicated time points, the mouse eyecups (RPE-choroid-sclera complex) were harvested and subjected to detection of DDR2 messenger RNA (mRNA) and protein expression by qPCR and immunoblot, respectively. We found that after 90-mW laser irradiation, both the mRNA and protein levels of DDR2 initially decreased and reached its lowest levels at day 3 and thereafter was followed by a small upregulation (Fig. 2a, b). In contrast, subthreshold laser treatment (40 mW) that failed to induce CNV had no effect on DDR2 expression (Fig. s1).

### The magnitude of experimental CNV was increased by a host deficiency of DDR2

In order to confirm the contribution of DDR2 to CNV formation, we compared the pathological severity in control and slie mice. The results of fundus fluorescein angiography (FFA) showed that, 2 weeks after laser photocoagulation, the *slie* group had more and larger areas of vascular leakage than control animals (Fig. 3a). H&E staining indicated that the length and thickness of CNV were also exaggerated in *slie* mice (Fig. 3b). Consistent to these results, the mean area and volume of CNV lesions in *slie* mice were much larger compared to wild-type ones, as

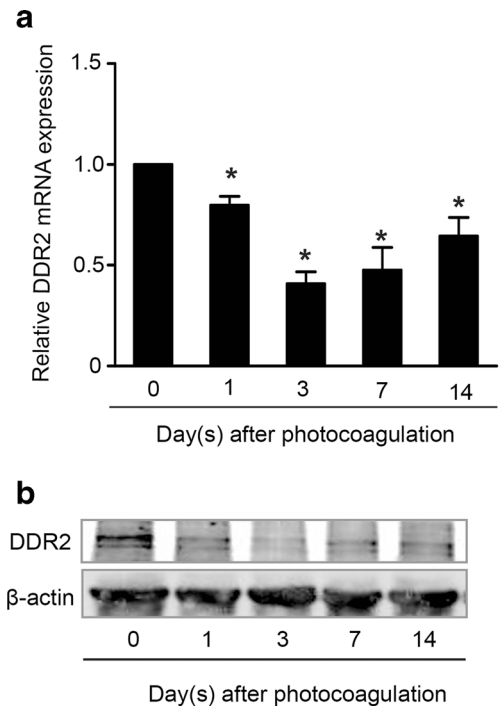


**Fig. 2** DDR2 expression in the mouse choroidal tissues was reduced by the induction of CNV. The eyes of wild-type C57/B16 mice were exposed to laser to induce CNV as described in "Materials and methods," and the eyecups were collected at the indicated day points after laser treatment (three mice for each group). The relative expression level of DDR2 mRNA (**a**) was determined by qPCR. *Gapdh* was used as an internal reference control. Bar graphs are the means±SD of three separate experiments. *$p<0.01$. The total protein homogenates (from three mice) taken at the indicated days (**b**) were loaded for immunoblot analysis of DDR2 protein. β-actin was used as a loading control

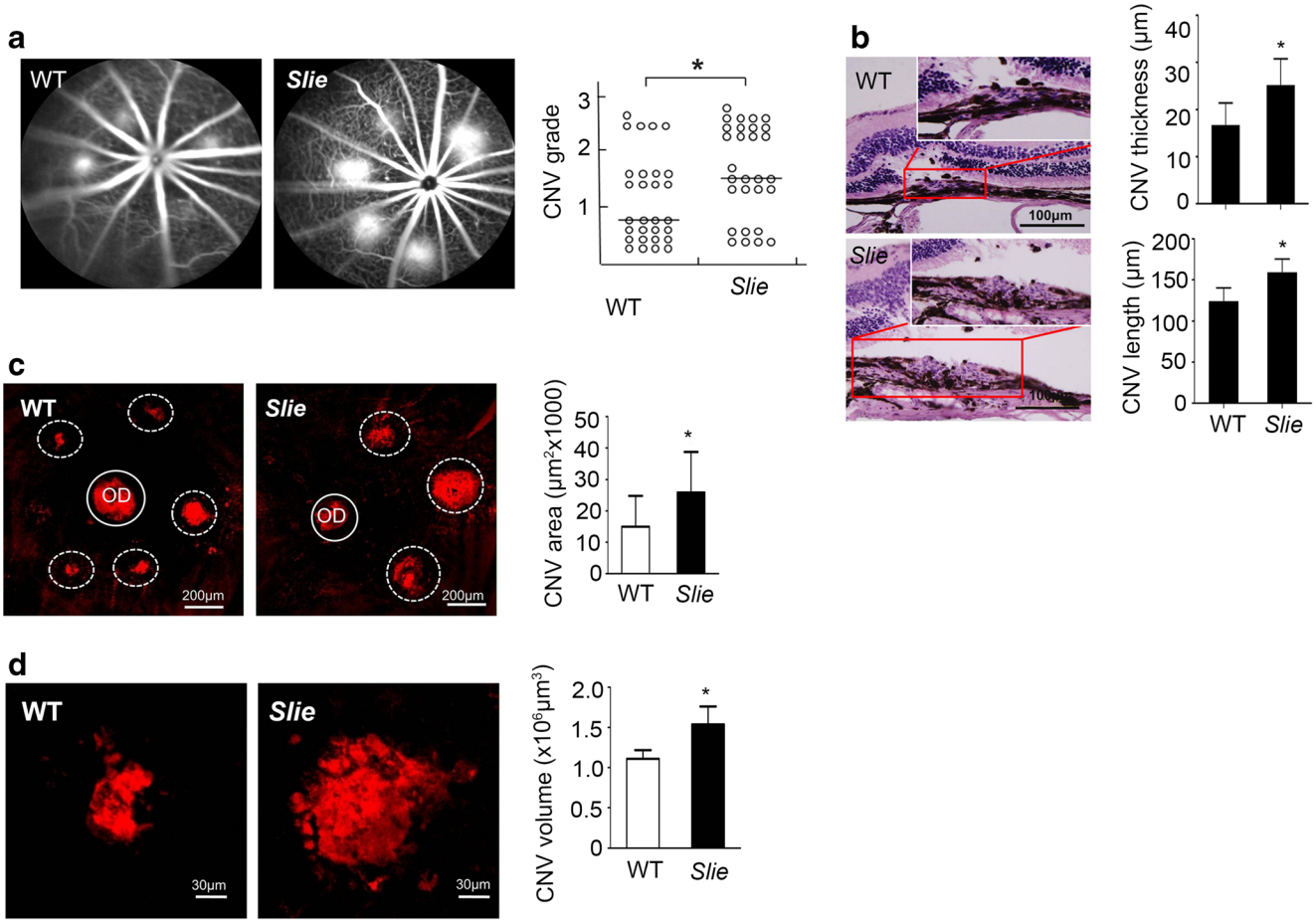


**Fig. 3** DDR2 deficient mice exhibited increased CNV severity. The eyes of wild-type or slie mutant mice (at least three mice for each group) were treated with laser coagulation, and 14 days later, the pathological status of the choroidal tissues were evaluated by FFA, H&E staining, and choroidal flat-mounts. FFA assay (**a**) showed more and larger area of leakage in slie group. CNV grade was scored as described in "Materials and methods." *Lines* in the dot chart indicate median leakage levels. Representative images of H&E staining (**b**). *Scale bar*, 100 μm. Histograms show the average thickness and length of CNV in ten randomly selected images. Choroidal flat-mount analysis (**c**) demonstrated enlarged area of CNV in slie mice. *Dotted circles* indicate area of CNV; *OD* indicates optic disc. *Scale bar*, 200 μm. Histogram shows the average area of CNV in ten randomly selected images. Three-dimensional reconstruction of choroidal flat-mount images (**d**). *Scale bar*, 30 μm. Histogram shows the average volume of CNV in ten randomly selected images. *$p<0.01$

demonstrated by choroid flat-mount analysis (Fig. 3c, d). These evidences collectively suggest that a host absence of DDR2 promoted the formation of experimental CNV.

## Intravitreous injection of DDR2 siRNA or DDR2-expressing adenovirus augments or alleviates the mouse responses to CNV induction

The above results urged us to further explore whether local alterations of DDR2 expression in the mouse eyes can similarly affect the pathogenesis of CNV. Firstly, we tried to downregulate DDR2 through intravitreous injection of our previously described DDR2 siRNA with high knockdown efficiency [20]. It was shown that the in vivo duration of DDR2 siRNA exhibited a time-dependent manner, as assayed by qPCR and immunoblot (Fig. 4a, b). Thus, in the subsequent experiment, the mice received siRNA treatment on the day of laser irradiation and the sizes of CNV lesions were evaluated at day 7 after photocoagulation. Compared to the scramble siRNA group, a single intraocular administration of DDR2 siRNA aggravated laser-

**Fig. 4** DDR2 siRNA treatment augments laser-induced CNV. C57BL/six ▶ mice received intravitreous injection of scramble siRNA or siRNA against DDR2 and at various time points after siRNA treatment, and the choroidal tissues from three mice were obtained and pooled together for qPCR (**a**) and immunoblot (**b**) analysis of DDR2 expression, respectively. The experiment was performed independently for at least three times. Twelve hours after sham or photocoagulation treatment, C57BL/six mice received injection of siRNAs and CNV were evaluated 7 days later. FFA assay (**c**). *Lines* in the dot chart indicate median leakage levels. Representative images of H&E staining (**d**). *Scale bar*, 100 μm. Histograms show the thickness and length of CNV. Choroidal flat-mount analysis (**e**). *Dotted circles* indicate area of CNV; *OD* indicates optic disc. *Scale bar*, 200 μm. Histogram shows the average area of CNV in ten fields. Representative three-dimensional reconstruction images of choroidal flat-mount (**f**). *Scale bar*, 30 μm. Histogram shows the average volume of CNV in ten fields. *$p<0.01$

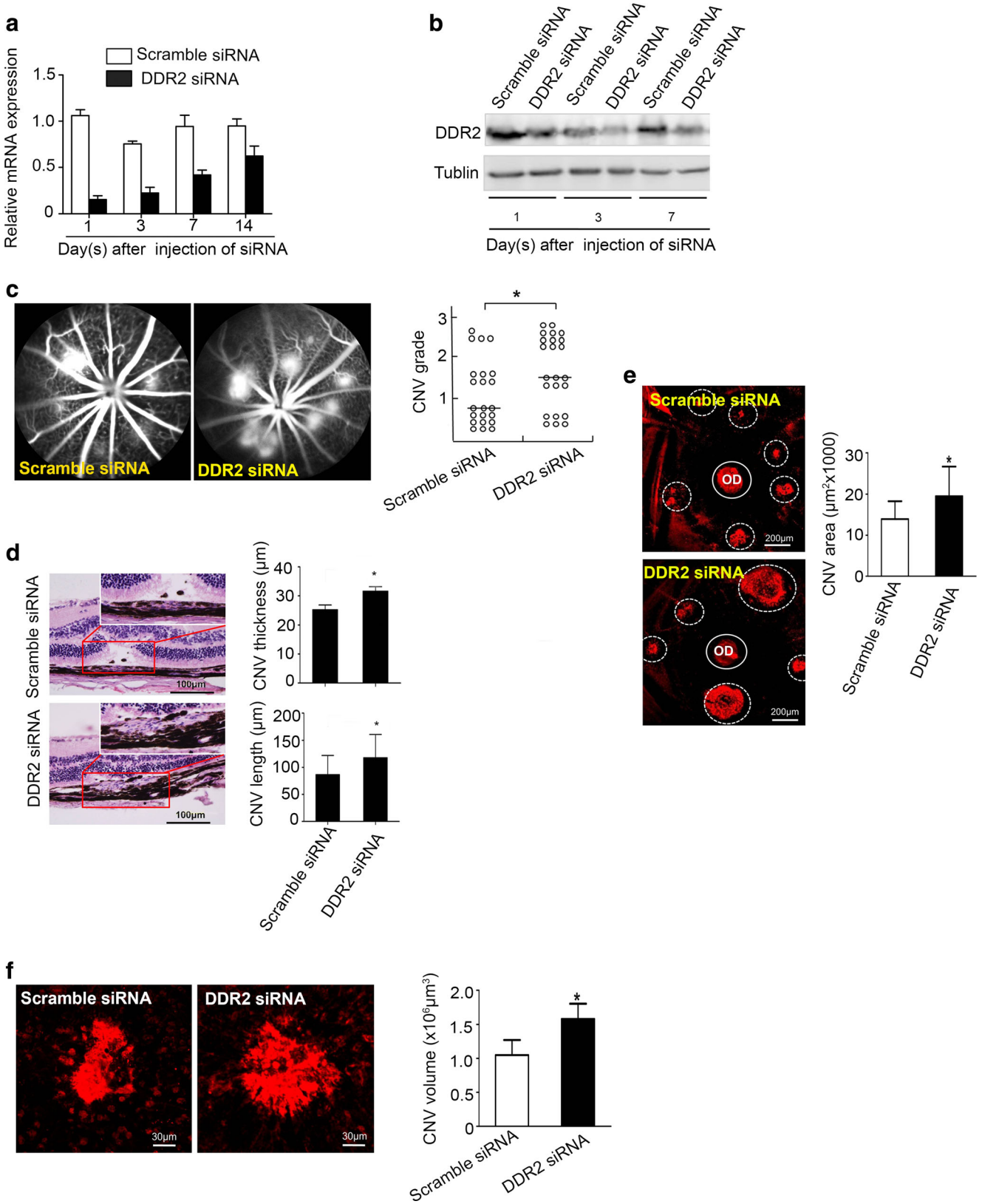


induced CNV in mice, as demonstrated by the results of FFA and choroid flat-mount (Fig. 4c–f).

Next, we boosted the expression of DDR2 through an adenovirus-mediated strategy. Immunoblot analysis showed

that the expression peak of Ad-DDR2 occurred at day 7 (Fig. 5a). To evaluate the in vivo distribution of recombinant protein, the mouse eye tissues were subjected to fluorescence microscopy for the detection of EGFP. It was demonstrated that, 7 days after infection, the EGFP fluorescence could be observed in multiple areas including RPE, choroid, retina nerve fiber layer, and ciliary body (Fig. s2), indicating a sustained expression of recombinant adenovirus throughout the active phase of CNV. By inducing CNV formation in EGFP- (control group) or DDR2-overexpressing animals, we found that enhanced expression of DDR2 significantly suppressed the choroidal angiogenic response (Fig. 5b–e).

## DDR2 induces changes in the expression levels of major pro-angiogenic factors in laser-injured choroidal tissues as well as in RPE cells

It is known that the angiogenic process is controlled in a carefully coordinated fashion by a variety of factors of which VEGF-A and angiopoietin (Ang)-2 play key pro-angiogenic roles [23, 24]. In order to elucidate how DDR2 loss enhances the severity of CNV, we analyzed the expression levels of the two factors in laser-irradiated choroidal tissues from control or *slie* mice by qPCR and immunoblot, respectively. It was demonstrated that upon CNV induction, the mutant mice had a higher levels of both VEGF-A and Ang-2 than the control group (Fig. 6a, b). Similar

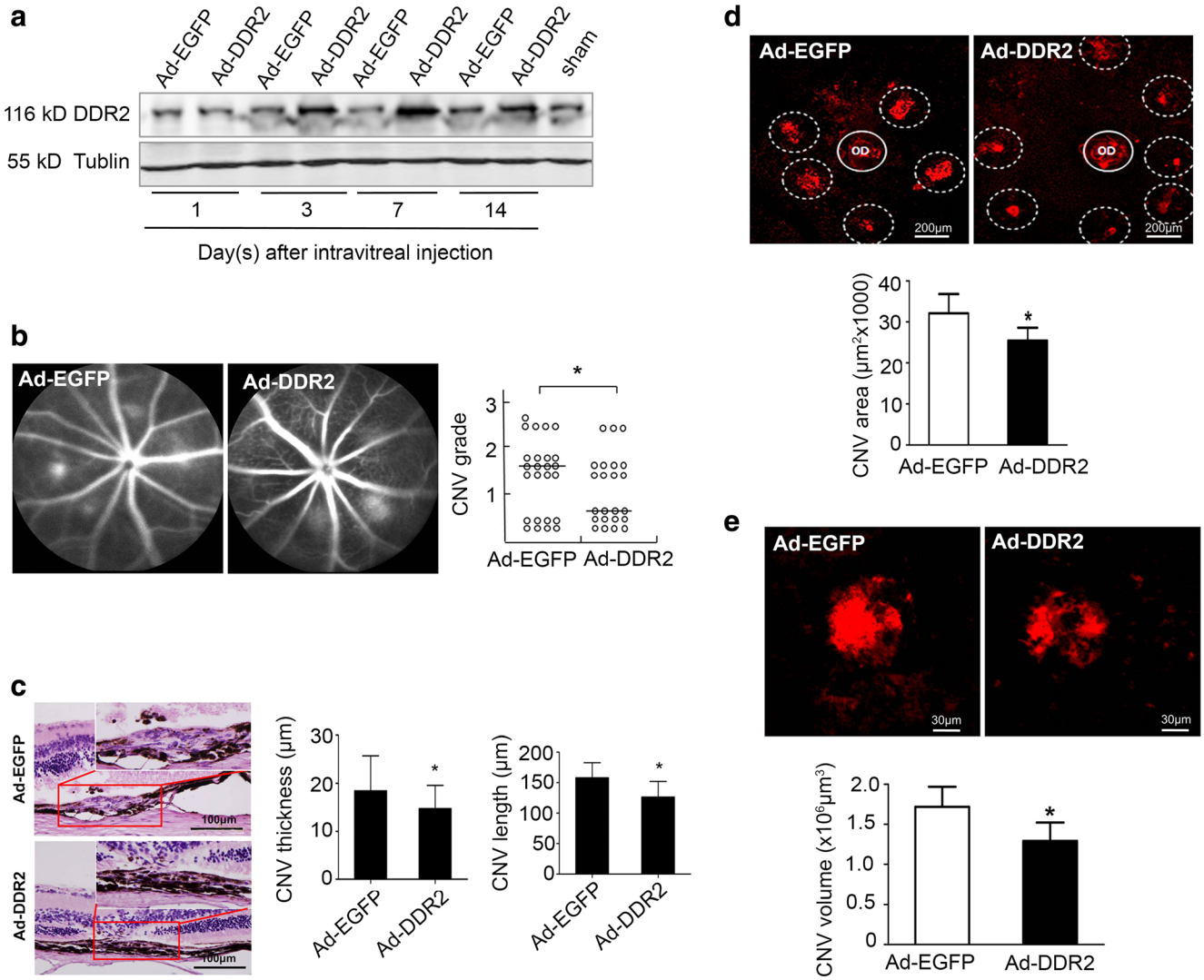


**Fig. 5** DDR2 overexpression reduces the severity of laser-induced CNV. Adenovirus-mediated expression of DDR2 in the mouse eye (**a**). C57BL/six mice were intravitreously administered adenovirus expressing either EGFP or DDR2, and the eye tissues were subjected to immunoblot analysis of DDR2 expression at the indicated days after adenovirus injection. Twelve hours after photocoagulation, C57BL/six mice received intravitreous injection of Ad-EGFP or Ad-DDR2 and CNV were evaluated 14 days later. FFA assay (**b**). *Lines* in the dot chart indicate median leakage levels. H&E staining (**c**). *Scale bar*, 100 μm. Histograms show the thickness and length of CNV. Choroidal flat-mount analysis (**d**). *Dotted circles* indicate area of CNV; *OD* indicates optic disc. *Scale bar*, 200 μm. Histogram shows the average area of CNV in ten fields. Representative three-dimensional reconstruction images of choroidal flat-mount (**e**). *Scale bar*, 30 μm. Histogram shows the average volume of CNV in ten fields. *$p<0.01$

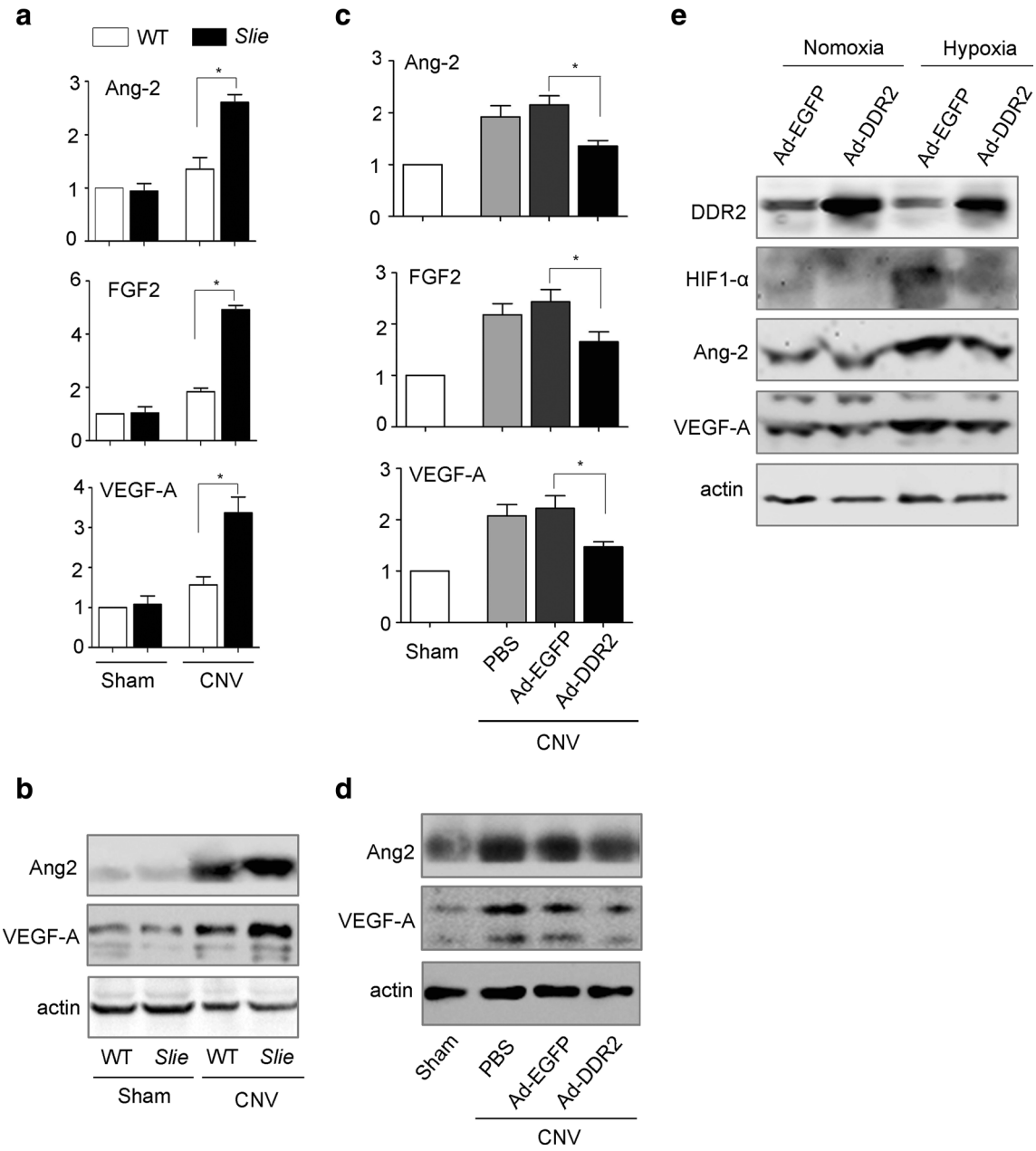


**Fig. 6** DDR2 controls the expression of pro-angiogenic growth factors involved in CNV genesis. The eyes of wild-type and slie mice were treated with or without laser photocoagulation, and 3 days later, the choroidal tissues from three mice were obtained and pooled together to analyze the mRNA expression of *Vegfa*, *Ang2*, and *Fgf2* by qPCR (**a**). The experiment was performed independently for at least three times. Sham group indicates non-lasered mice. The relative levels of mRNA were normalized to *Gapdh*. Fold induction of wild-type sham group was arbitrarily set as 1. *$p<0.01$. The samples in (**a**) were subjected to immunoblot analysis (**b**) of the protein expression VEGF-A and Ang-2. Twelve hours after photocoagulation, C57BL/six mice received intravitreous injection of Ad-EGFP or Ad-DDR2 and 3 days later (**c**, **d**), the mRNA and protein expression of the indicated angiogenic factors were examined. *$p<0.01$. Human RPE cell line ARPE19 was infected with Ad-EGFP or Ad-DDR2 for 24 h, and the cells were then cultured under nomoxia or hypoxia conditions for another 24 h. The expression levels of the indicated proteins were analyzed by immunoblot (**e**)

results were also observed when DDR2 was knocked down in wild-type C57/B16 mice using siRNA (Fig. s3a, b). Conversely, the introduction of DDR2-expressing adenovirus led to an inhibitory effect on their expression (Fig. 6c, d).

Increasing evidence suggests that RPE cells play a key role in the pathogenesis of CNV [25, 26], and this type of cells can secrete multiple angiogenic growth factors [6]. Thus, we performed in vitro experiments to examine whether DDR2 regulates the expression of VEGF and Ang-2 in human RPE cells. Because both VEGF and Ang-2 are hypoxia-inducible genes, we cultured Ad-DDR2-transduced ARPE19 cells under 3 % oxygen conditions for 24 h before immunoblot

analysis of the expression of the two angiogenic proteins. We found that in EGFP-expressing cells, low oxygen treatment resulted in dramatic increases in the expression levels of VEGF-A and Ang-2 as well as the hypoxic marker hypoxia-inducible factor (HIF)-1α. Consistent with the in vivo observation, the hypoxia-induced upregulation of these molecules was inhibited by enhanced expression of DDR2 (Fig. 6e). Since both VEGF and Ang-2 can stimulate the activation of PI3K/Akt/mTOR cascade in endothelial cells [27–30], we attempted to investigate whether the activation status of this pathway during CNV process was similarly affected by DDR2. In the ocular tissues of wild-type mice, laser treatment greatly increased the phosphorylation levels of Akt and mTOR, which was decreased by the intravitreal injection of PI3K inhibitor LY294002. The CNV-triggered activation of Akt and mTOR in DDR2 mutant mice was much higher than those in control mice (Fig. 7a). In support of these results, the activities of the two kinases under CNV conditions were augmented by DDR2 knockdown but attenuated by its overexpression (Figs. s4 and 7b). These molecular evidences strongly support the data from functional studies.

## Discussion

In this study, we reported that DDR2 deficiency in mice accelerates the induction of laser-induced CNV. The inhibitory role of DDR2 in the pathogenesis of CNV was additionally confirmed by use of DDR2 knockdown and overexpression strategies. In addition, we demonstrated that DDR2 negatively regulates the expression of several major pro-angiogenic factors in the laser-injured choroid as well as in RPE cells. To our knowledge, this represents the first investigation of DDR2 function in ocular disease.

The results from this study agree with the recent observation that DDR2 deficiency resulted in enhanced tumor angiogenesis in liver as well as increased VEGF expression in tumor-derived hepatic stellate cells (HSCs) [13]. In contrast to exhibiting an anti-angiogenic effect in choroidal and hepatic tissues, DDR2 was found to facilitate both VEGF- and tumor-induced angiogenesis within dermal environment [17]. These conflicting data strongly suggest that the specific pathological conditions with diverse types of DDR2-expressing angiogenic cells may determine the final influence of DDR2 signaling on neovascularization.

The cells that are involved in the development of CNV at least include choroidal endothelial cells (CECs), RPEs, and inflammatory cells. During CNV, CECs can undergo transition from a quiescent to an activated state in the presence of pro-angiogenic factors that are predominantly released by RPE cells and then acquire the ability to penetrate RPE layer and Bruch's membrane [25, 31]. As for the role of DDR2 in ECs, our recently published data have disclosed that enhanced expression of DDR2 increases the angiogenic activities of human umbilical vein endothelial cells (HUVECs) [17]. Conversely, the current study revealed that DDR2 inhibits the expression of VEGF-A and Ang-2 in RPE cells (Fig. 6e). Considering that VEGF-A and Ang-2 are potent angiogenic stimulators, it is likely that the positive regulation of DDR2 on endothelial proliferation and migration

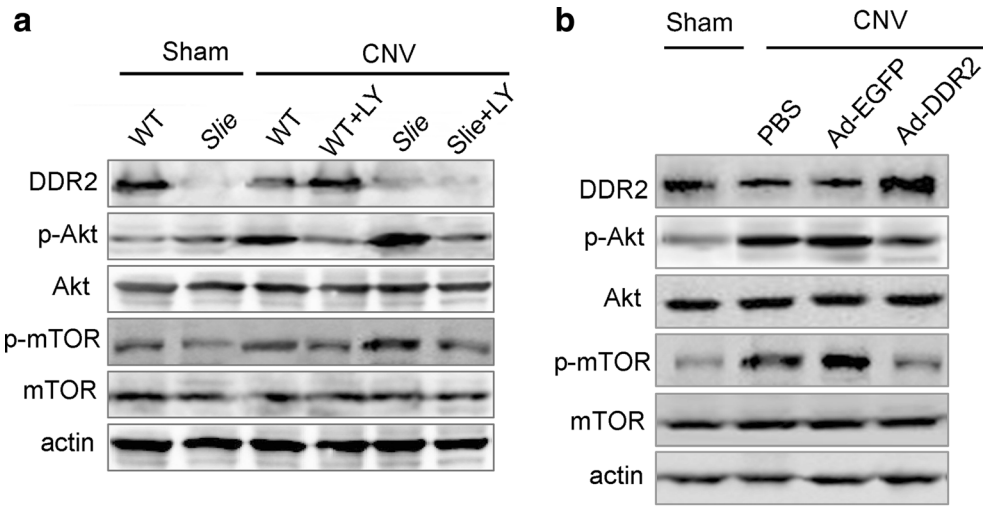


**Fig. 7** The activities of PI3K pathway after laser burn are altered by DDR2 downregulation or upregulation. The effect of DDR2 deficiency on CNV-induced activation of PI3K pathway (**a**). Twelve hours after sham (non-lasered) or laser treatment, wild-type or slie mice were administered with either DMSO or PI3K inhibitor LY294002 intravitreously. Three days later, the protein extracts from RPE-choroid-sclera complex (three mice each group) were prepared for immunoblot analysis of the phosphorylation levels of Akt and mTOR. The effect of enhanced expression of DDR2 on CNV-induced activation of PI3K pathway (**b**). Twelve hours after laser treatment, C57BL/six mice received intravitreous injection of Ad-EGFP or Ad-DDR2 and 3 days later, the protein extracts from RPE-choroid-sclera complex were subjected to immunoblot analysis

has been over balanced out by its negative modulation on RPE cell secretion of the two cytokines, finally making DDR2 give rise to an overall inhibitory outcome in choroidal angiogenesis. In addition to RPE cells, we do not exclude the possibility that dendritic cells (DCs) may also partially mediate the suppressive effect of DDR2 on CNV because DDR2 knockdown prevents the activation of DCs [32], and only immature DCs enhance CNV size [33]. Taking these evidences together, it is reasonable to believe that DDR2 attenuation of CNV formation might be predominantly achieved through its negative control of the pro-angiogenic activities of RPE cells and DCs.

By comparing the expression level of DDR2 at various time points after the development of laser-induced CNV, we found that both the mRNA and protein levels of DDR2 initially decreased and thereafter gradually increased. The initial downregulation may be caused by the laser damage to the resident cells that express DDR2 such as RPE cells and fibroblasts. The latter upregulation may be related to either the increased recruitment of other types of DDR2-expressing cells from bone marrow such as endothelial cells and DCs, or the occurrence of hypoxic conditions that were shown to enhance the expression of DDR2 [17, 34].

An interesting finding in this report is that DDR2 overexpression abrogates the expression of HIF-1α as well as its downstream target genes VEGF-A and Ang-2 in hypoxia-treated RPE cells. In fact, DDR2 inhibition of VEGF expression has been previously documented in tumor-derived HSCs [13]. However, in hepatocellular carcinoma cells, DDR2 knockdown was linked to reduced trans-activation of HIF-1α and diminished expression of VEGF [35]. Thus, it appears that DDR2 exhibits opposite effects on the expression of VEGF in different types of cells. The detailed mechanisms underlying DDR2 control of HIF-1α activity as well as the expression of its target genes needs to be investigated in future studies.

It has been well established that VEGF regulates endothelial cell survival through the PI3K/Akt signal transduction pathway. Our previous study has also shown that the PI3K pathway is activated during the early phase of CNV formation and PI3K inhibition can lead to significant suppression of experimental CNV [21]. Here, we found that the CNV-triggered activation of Akt and mTOR in the choroidal tissues had an inverse relationship with the expression level of DDR2, which is perfectly in agreement with the results that DDR2 suppresses the expression of VEGF-A in the laser-injured choroid as well as in RPE cells. As a result, the potential mechanism underlying DDR2 suppression of CNV can be hypothesized as follows: during the pathogenesis of CNV, DDR2 inhibits the expression of pro-angiogenic cytokines by RPE cells, which in turn hampers the endothelial proliferation and survival.

In conclusion, our studies identified an anti-angiogenic role of DDR2 in laser-induced CNV. These studies may suggest DDR2 as a potential new target for the prevention of human pathological ocular neovascularization.

**Acknowledgments** We greatly thank Dr. Wei Zhang (The Fourth Military Medical University, Xi'an, China) for providing us the DDR2-expressing adenovirus stock.

**Funding** This work was supported by the National Natural Science Foundation of China (81070748, 81000392) and grants from the Chinese National Key Basic Research and Development Program (2011CB510200 and 2010CB529705).

**Conflict of interest** The authors declare no competing or financial interests.

## References

1. Calabrese A, Bernard JB, Hoffart L, Faure G, Barouch F, Conrath J, Castet E (2011) Wet versus dry age-related macular degeneration in patients with central field loss: different effects on maximum reading speed. Invest Ophthalmol Vis Sci 52:2417–2424
2. Campochiaro PA (2000) Retinal and choroidal neovascularization. J Cell Physiol 184:301–310
3. Torres RJ, Maia M, Muccioli C, Winter G, Souza GK, Pasqualotto LR, Luchini A, Precoma DB (2009) Modifiable risk factors for age-related macular degeneration. Arq Bras Oftalmol 72:406–412
4. Campa C, Costagliola C, Incorvaia C, Sheridan C, Semeraro F, De Nadai K, Sebastiani A, Parmeggiani F (2010) Inflammatory mediators and angiogenic factors in choroidal neovascularization: pathogenetic interactions and therapeutic implications. Mediat Inflamm 2010
5. Shi X, Semkova I, Muther PS, Dell S, Kociok N, Joussen AM (2006) Inhibition of TNF-alpha reduces laser-induced choroidal neovascularization. Exp Eye Res 83:1325–1334
6. Krzystolik MG, Afshari MA, Adamis AP, Gaudreault J, Gragoudas ES, Michaud NA, Li W, Connolly E, O'Neill CA, Miller JW (2002) Prevention of experimental choroidal neovascularization with intravitreal anti-vascular endothelial growth factor antibody fragment. Arch Ophthalmol 120:338–346
7. Lazic R, Gabric N (2007) Intravitreally administered bevacizumab (Avastin) in minimally classic and occult choroidal neovascularization secondary to age-related macular degeneration. Graefes arch Clin Exp Ophthalmology=Albrecht von Graefes Archiv fur klin Exp Ophthalmol 245:68–73
8. Barber NA, Ganti AK (2011) Pulmonary toxicities from targeted therapies: a review. Target Oncol 6:235–243
9. Buyukoglan H, Gulmez I, Tutar N, Oymak FS, Kanbay A, Demir R (2011) Gluteal abscess: an unusual complication of Bacille Calmette-Guerin. Anna Thorac Med 6:235–236
10. Obayashi Y, Yamadori I, Fujita J, Yoshinouchi T, Ueda N, Takahara J (1997) The role of neutrophils in the pathogenesis of idiopathic pulmonary fibrosis. Chest 112:1338–1343
11. Vogel W, Gish GD, Alves F, Pawson T (1997) The discoidin domain receptor tyrosine kinases are activated by collagen. Mol Cell 1:13–23
12. Vogel WF, Abdulhussein R, Ford CE (2006) Sensing extracellular matrix: an update on discoidin domain receptor function. Cell Signal 18:1108–1116
13. Badiola I, Olaso E, Crende O, Friedman SL, Vidal-Vanaclocha F (2012) Discoidin domain receptor 2 deficiency predisposes hepatic tissue to colon carcinoma metastasis. Gut 61:1465–1472

14. Olaso E, Arteta B, Benedicto A, Crende O, Friedman SL (2011) Loss of discoidin domain receptor 2 promotes hepatic fibrosis after chronic carbon tetrachloride through altered paracrine interactions between hepatic stellate cells and liver-associated macrophages. Am J Pathol 179:2894–2904
15. Olaso E, Lin HC, Wang LH, Friedman SL (2011) Impaired dermal wound healing in discoidin domain receptor 2-deficient mice associated with defective extracellular matrix remodeling. Fibrogenesis Tissue Repair 4:5
16. Xu L, Servais J, Polur I, Kim D, Lee PL, Chung K, Li Y (2010) Attenuation of osteoarthritis progression by reduction of discoidin domain receptor 2 in mice. Arthritis Rheum 62:2736–2744
17. Zhang S, Bu X, Zhao H, Yu J, Wang Y, Li D, Zhu C, Zhu T, Ren T, Liu X et al (2014) A host deficiency of discoidin domain receptor 2 (DDR2) inhibits both tumour angiogenesis and metastasis. J Pathol 232:436–448
18. Kano K, Marin de Evsikova C, Young J, Wnek C, Maddatu TP, Nishina PM, Naggert JK (2008) A novel dwarfism with gonadal dysfunction due to loss-of-function allele of the collagen receptor gene, Ddr2, in the mouse. Mol Endocrinol 22:1866–1880
19. Kim LG, Thompson SG, Marteau TM, Scott RA, Multicentre Aneurysm Screening Study G (2004) Screening for abdominal aortic aneurysms: the effects of age and social deprivation on screening uptake, prevalence and attendance at follow-up in the MASS trial. J Med Screen 11:50–53
20. Zhang Y, Su J, Yu J, Bu X, Ren T, Liu X, Yao L (2011) An essential role of discoidin domain receptor 2 (DDR2) in osteoblast differentiation and chondrocyte maturation via modulation of Runx2 activation. J Bone Miner Res 26:604–617
21. Yang XM, Wang YS, Zhang J, Li Y, Xu JF, Zhu J, Zhao W, Chu DK, Wiedemann P (2009) Role of PI3K/Akt and MEK/ERK in mediating hypoxia-induced expression of HIF-1alpha and VEGF in laser-induced rat choroidal neovascularization. Invest Ophthalmol Vis Sci 50:1873–1879
22. Li X, Cai Y, Wang YS, Shi YY, Hou W, Xu CS, Wang HY, Ye Z, Yao LB, Zhang J (2012) Hyperglycaemia exacerbates choroidal neovascularisation in mice via the oxidative stress-induced activation of STAT3 signalling in RPE cells. PLoS One 7:e47600
23. Monteagudo B, Labandeira J, Cabanillas M, Acevedo A, Leon-Muinos E, Toribio J (2012) Prevalence of milia and palatal and gingival cysts in Spanish newborns. Pediatr Dermatol 29:301–305
24. Zhang Y, Tanner KE (2008) Effect of filler surface morphology on the impact behaviour of hydroxyapatite reinforced high density polyethylene composites. J Mater Sci Mater Med 19:761–766
25. Campochiaro PA, Soloway P, Ryan SJ, Miller JW (1999) The pathogenesis of choroidal neovascularization in patients with age-related macular degeneration. Mol Vis 5:34
26. Nowak JZ (2006) Age-related macular degeneration (AMD): pathogenesis and therapy. Pharmacol Rep: PR 58:353–363
27. Gerber HP, McMurtrey A, Kowalski J, Yan M, Keyt BA, Dixit V, Ferrara N (1998) Vascular endothelial growth factor regulates endothelial cell survival through the phosphatidylinositol 3-kinase/Akt signal transduction pathway. Requirement for Flk-1/KDR activation. J Biol Chem 273:30336–30343
28. Gille H, Kowalski J, Yu L, Chen H, Pisabarro MT, Davis-Smyth T, Ferrara N (2000) A repressor sequence in the juxtamembrane domain of Flt-1 (VEGFR-1) constitutively inhibits vascular endothelial growth factor-dependent phosphatidylinositol 3-kinase activation and endothelial cell migration. EMBO J 19:4064–4073
29. Maliba R, Lapointe S, Neagoe PE, Brkovic A, Sirois MG (2006) Angiopoietins-1 and −2 are both capable of mediating endothelial PAF synthesis: intracellular signalling pathways. Cell Signal 18: 1947–1957
30. Wu X, Liu N (2010) The role of Ang/Tie signaling in lymphangiogenesis. Lymphology 43:59–72
31. Samalavichius NE (2004) [Preventive Turnbull ileostomy]. Khirurgiia (Mosk):50–52
32. Lee JE, Kang CS, Guan XY, Kim BT, Kim SH, Lee YM, Moon WS, Kim DK (2007) Discoidin domain receptor 2 is involved in the activation of bone marrow-derived dendritic cells caused by type I collagen. Biochem Biophys Res Commun 352:244–250
33. Baxa U, Taylor KL, Steven AC, Wickner RB (2004) Prions of saccharomyces and Podospora. Contrib Microbiol 11:50–71
34. Chen SC, Wang BW, Wang DL, Shyu KG (2008) Hypoxia induces discoidin domain receptor-2 expression via the p38 pathway in vascular smooth muscle cells to increase their migration. Biochem Biophys Res Commun 374:662–667
35. Lee NO, Park JW, Lee JA, Shim JH, Kong SY, Kim KT, Lee YS (2012) Dual action of a selective cyclooxygenase-2 inhibitor on vascular endothelial growth factor expression in human hepatocellular carcinoma cells: novel involvement of discoidin domain receptor 2. J Cancer Res Clin Oncol 138:73–84